# FIELD OBSERVATIONS AND NUMERICAL MODELING OF SWASH TRANSFORMATION IN THE PRESENCE OF AN ARTIFICIAL VEGETATION PATCH

Magsood Mansur, Northeastern University, mansur.m@northeastern.edu; Qin Chen, Northeastern University, q.chen@northeastern.edu; Julia Hopkins, Northeastern University, ju.hopkins@northeastern.edu; Reza Salatin, Woods Hole Oceanographic Institution, reza.salatin@whoi.edu; Tyler McCormack, Northeastern University, mccormack.ty@northeastern.edu; Patrick Dickhudt, US Army Corps of Engineers, Field Research Facility, patrick.j.dickhudt@erdc.dren.mil

## INTRODUCTION

Global climate change and sea level rise pose a dire threat to life and property of coastal communities. Vegetation has been shown to act as a vanguard against coastal hazards in the nearshore regions by attenuating wave energy, reducing storm surges, and preventing erosion (Jadhav et al., 2013; Zhu et al., 2023). To improve our understanding of wave-beach-vegetation interaction, we conducted a field experiment at the US Army Corps of Engineers' Field Research Facility (FRF) in Duck, North Carolina, as part of the DUNEX (DUring Nearshore Event eXperiment). We installed a patch of artificial vegetation in the swash zone to test how beach vegetation attenuates wave energy and subsequently how it might reduce erosion. In this study, field observations and field validated numerical modeling are integrated to understand the swash energy reduction in the presence of an artificial vegetation patch. We investigate (1) the wave transformation in the swash zone in the presence of the artificial vegetation patch, (2) the vegetation drag coefficient in the swash zone, and (3) the wave energy attenuation due to the presence of the artificial vegetation patch in the swash zone.

## METHODOLOGY

We installed a 5m x 5m artificial vegetation patch made of nylon 6/6 cable ties, 33 cm long and 0.5 cm wide, in the swash zone about 100 m to the south of the FRF pier on September 23, 2021. We deployed an array of instruments along a cross-shore transect through the centerline of the patch consisting of four RBR depth (pressure) loggers, three Nortek Vector acoustic Doppler velocimeters (ADVs), one Nortek Signature1000 acoustic Doppler current profiler (ADCP) and seven GoPro cameras (Figure 1a; Figure 1b). We set up another instrumented reference cross-shore transect about 5m from the south edge of the patch consisting of four RBR depth (pressure) loggers, two SonTek current meters and one GoPro camera (Figure 1b).

The RBRs measured a continuous time series of pressure sampling at 8 Hz. The data were converted to water depth and free surface elevation (Raubenheimer, 2002). For the present study we were only interested in the two RBRs that were at the leading and trailing edge of the vegetation patch (RBR 2 and RBR 3 in Figure 1b) and the two corresponding RBRs in the reference transect (RBR 6 and RBR 7 in Figure 1b). These RBRs only underwent episodic continuous submergence. We considered only those periods of continuously submerged data for this study. We analyzed the data to compute the mean water depth $h$ and significant wave/swash height $H_s$ ($= 4\sigma$, where $\sigma$ represents the standard deviation of the water surface elevation fluctuations obtained from the pressure data) (Raubenheimer, 2002). We computed the root-mean square wave/swash height $H_{rms}$ assuming Rayleigh distribution (Jadhav et al, 2013). We then quantified the percentage of the characteristic wave height reduction ($H_{rms}$ for random waves) across the vegetation transect and the reference transect to identify if the vegetation caused more wave height attenuation as compared to the unvegetated reference transect.


Figure 1 – (a) The instrumented (mounted by the poles) artificial vegetation patch (marked by the safety flags) on the FRF beach to the south of the research pier on the background. (b) Schematic diagram of the instrument setup. Each shape and color represent the instruments as follow: green square – artificial vegetation patch; yellow circle – RBR; red triangle – Nortek ADV; pink triangle – SonTek ADV; purple diamond – ADCP; light blue cross – 2 GoPro cameras mounted on a T-section; dark blue cross – 1 GoPro. The bottom left corner has images of the Nortek ADV (top left), RBR (top right), ADCP (bottom right) and GoPro (bottom left) that were being used for the fieldwork.

Many field and laboratory studies of wave height attenuation by vegetation used the wave energy balance equation to infer the vegetation drag coefficient $C_D$, which cannot be measured directly from the field (Jadhav et al., 2013). There are several approaches to determine $C_D$. Most of the studies calibrated $C_D$ from wave height

reduction based on theoretical wave dissipation model. A recent study incorporated the influence of vegetation flexibility through effective plant height and determined a species-independent $C_D$ formula for salt marshes in random waves based on three independent datasets that covered a wide range of hydrodynamic conditions and vegetation traits (Zhu et al., 2023). The present study is built upon the approach therein. We extended their approach to the swash region by replacing the orbital velocities obtained from the linear theory with orbital velocities for nonlinear waves in the swash zone which are strongly correlated to $\sqrt{gh}$ (Raubenheimer, 2002).

The wave transformation along a cross-shore transect is governed by the 1D energy balance equation:

$$\frac{\partial EC_g}{\partial x} = -D_b - D_f \quad (1)$$

where, $E$ is the wave energy density which is equal to $1/8\,\rho g H_{rms}^2$, $C_g$ is the group velocity, the direction of $x$ coordinate is positive along the direction of wave propagation, and $D_b$ and $D_f$ are time-averaged energy dissipation rate per unit horizontal area due to wave breaking and bottom friction respectively. In the presence of vegetation, the time-averaged energy dissipation rate per unit horizontal area due to vegetation, $D_v$ is included in Eq. 1 as follows:

$$\frac{\partial EC_g}{\partial x} = -D_b - D_f - D_v \quad (2)$$

The formulations for $D_b$, $D_f$, and $D_v$ were applied in this study as follows (Thornton & Guza, 1983; Janssen & Battjes, 2007; Roelvink et al., 2010; Jadhav et al., 2013; Wang et al., 2022; Zhu et al., 2023):

$$D_b = \frac{3\sqrt{\pi}\alpha_b^3 f \rho g H_{rms}^3}{16h} Q_b \quad (3)$$

$$D_f = 0.28\rho f_0 u_0^3 \quad (4)$$

$$D_v = \frac{1}{2\sqrt{\pi}} \rho C_D b_v N_v \left(\frac{\sigma}{2}\right)^3 \frac{(\sinh k\alpha h)^3 + 3\sinh k\alpha h}{3k(\sinh kh)^3} H_{rms}^3 \quad (5)$$

where, $\rho$ is the water density, $g$ is the acceleration due to gravity, $\alpha_b$ is the wave dissipation coefficient determined from the field data, $Q_b$ is the fraction of breaking waves, $f$ is the frequency, $f_0$ is the bottom friction coefficient, $u_0$ is the orbital velocity amplitude, $b_v$ is the width or diameter of the stem, $N_v$ is the population density, $\alpha$ is the ratio of vegetation height $h_v$ to $h$, $k$ is the wave number, and $\sigma$ is the wave angular frequency.

Equations 1-5 were solved by the finite difference method to obtain the spatial variations of $H_{rms}$. $H_{rms}$ values at the leading edge of the vegetation patch provided the boundary conditions, with grid size being set as 0.01 m. The numerical solutions to Eq. 1 gave the wave height reduction due to breaking and bottom friction whereas the numerical solutions to Eq. 2 gave the wave height reduction due to the combined effects of breaking, bottom friction, and vegetation.

## RESULTS

We obtained $H_{rms}$ measurements and calculated the percentage of reduction rates. Average $H_{rms}$ reduction per meter increased over the vegetation transect as compared to the unvegetated reference transect (Figure 2). On average, the increase in $H_{rms}$ attenuation per meter over the vegetation transect varied from 15.85% (on October 8, 2021) to 32.48% (on October 9, 2021) (Figure 2).

Using the finite difference method, we solved Eq. 1 for $H_{rms}$ at each $x$ grid and iteratively calibrated the wave dissipation coefficient $\alpha_b$ along the reference transect by using the bisection method until the error between the observed and modeled $H_{rms}$ is less than 2%. Using these calibrated $\alpha_b$ values we then solved Eq. 2 for $H_{rms}$ and iteratively calibrated the vegetation drag coefficient $C_D$ along the vegetation transect by using the bisection method until the error between the observed and modeled $H_{rms}$ is less than 2%. We found the relationship between $C_D$ and $Re$ based on the definition of $Re$ which is given by $Re = \frac{b_v u_b}{\nu}$, where $u_b$ is the maximum near-bed orbital velocity at the leading edge of vegetation and $\nu$ is the kinematic viscosity of water. Finally, we compared the amount of swash energy dissipation due to breaking, bottom friction and vegetation, respectively.

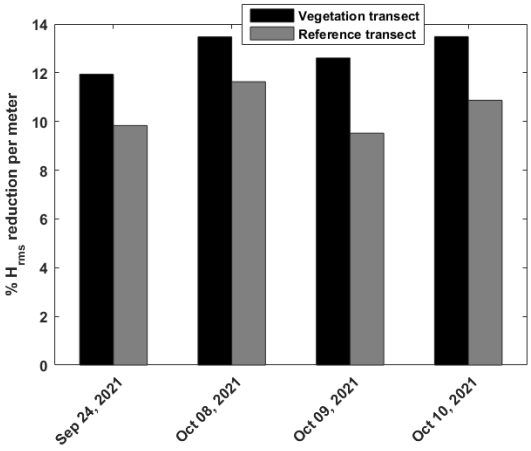


Figure 2 – Percentage of $H_{rms}$ reduction per meter across the vegetation and reference transects averaged over a day.

## REFERENCES


Jadhav, Chen, & Smith (2013): Spectral distribution of wave energy dissipation by salt marsh vegetation, Coastal Engineering, vol. 77, pp.99-107.

Janssen & Battjes (2007): A note on wave energy dissipation over steep beaches, Coastal Engineering, vol. 54(9), pp.711-716.

Raubenheimer (2002): Observations and predictions of fluid velocities in the surf and swash zones, Journal of Geophysical Research: Oceans, vol. 107(C11), pp.11-1.

Roelvink, Reniers, Van Dongeren, de Vries, Lescinski, & McCall (2010): XBeach model description and manual, Unesco-IHE Institute for Water Education, Deltares and Delft Univ. of Technology, Report June, 21, 2010.

Thornton & Guza (1983): Transformation of wave height distribution. Journal of Geophysical Research: Oceans, vol. 88(C10), pp.5925-5938.

Wang, Chen, & Chen (2022): Reconstruction of nearshore wave fields based on physics-informed neural networks, Coastal Engineering, vol. 176, p.104167.

Zhu, Chen, Ding, Jafari, Wang & Johnson (2023): Towards a unified drag coefficient formula for quantifying wave energy reduction by salt marshes, Coastal Engineering, vol. 180, p.104256.